hLife

ARTICLE

Targeted protein editing technique in living mammalian cells by peptide-fused PNGase

Min Wu[1,2,#], Guijie Bai[1,#], Ziyi Zhang[1,3], Haixia Xiao[2,4], Wenliang Sun[1,2], Chaoguang Tian[1,2,*]

*Correspondence: tian_cg@tib.cas.cn (C.T.)
Received: April 26, 2024; Revised: July 5, 2024; Accepted: July 7, 2024
Doi:10.1016/j.hlife.2024.07.003

Citation: Wu M, Bai G, Zhang Z, et al. Targeted protein editing technique in living mammalian cells by peptide-fused PNGase. *hLife* 2024;■:1–16.

GRAPHICAL ABSTRACT

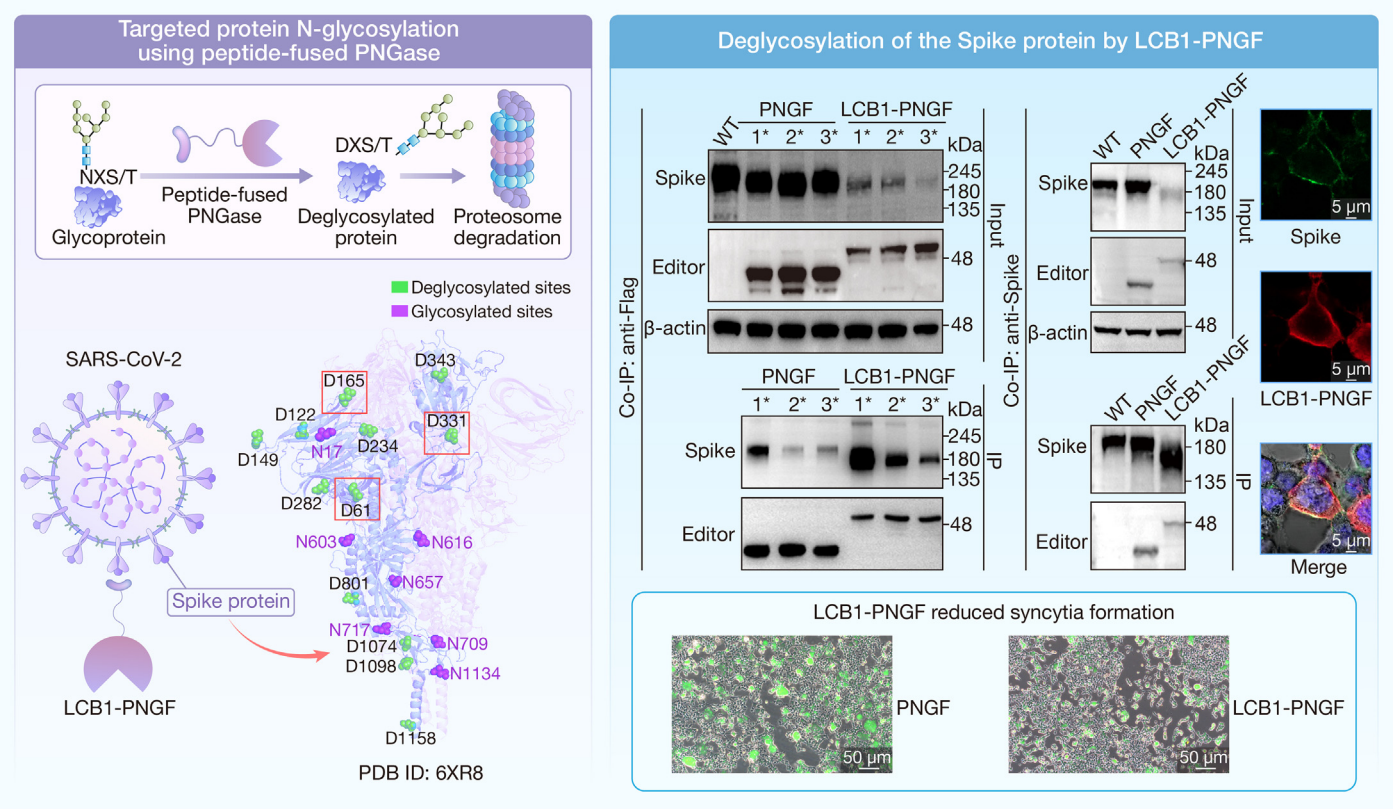

HIGHLIGHTS

- **Peptide-fused peptide:N-glycanase (PNGase) targets and edits N-glycosylated proteins of interest in living cells.**
- **The targeted deglycosylation and deamidation editing significantly decreased protein stability and accelerated degradation.**
- **LCB1- PNGase F (PNGF) edited SARS-CoV-2 spike protein and substantially reduced syncytia formation and virus entry.**

ARTICLE

Targeted protein editing technique in living mammalian cells by peptide-fused PNGase

Min Wu[1,2,#], Guijie Bai[1,#], Ziyi Zhang[1,3], Haixia Xiao[2,4], Wenliang Sun[1,2], Chaoguang Tian[1,2,*]

[1]Key Laboratory of Engineering Biology for Low-carbon Manufacturing, Tianjin Institute of Industrial Biotechnology, Chinese Academy of Sciences, Tianjin, China
[2]National Technology Innovation Center of Synthetic Biology, Tianjin, China
[3]School of Pharmaceutical Sciences, Jilin University, Jilin, China
[4]Laboraroty of Protein Engineering and Vaccines, Tianjin Institute of Industrial Biotechnology, Chinese Academy of Sciences, Tianjin, China
[#]These authors contributed equally to this work
*Correspondence: tian_cg@tib.cas.cn (C.T.)
Received: April 26, 2024; Revised: July 5, 2024; Accepted: July 7, 2024
Doi:10.1016/j.hlife.2024.07.003

Citation: Wu M, Bai G, Zhang Z, et al. Targeted protein editing technique in living mammalian cells by peptide-fused PNGase. *hLife* 2024;■:1–16.

ABSTRACT

Various precise gene editing techniques at the DNA/RNA level, driven by clustered regularly interspaced short palindrome repeats (CRISPR)/CRISPR-associated protein 9 (Cas9) technology, have gained significant prominence. Yet, research on targeted protein editing techniques remains limited. Only a few attempts have been made, including the use of specific proteases and de-O-glycosylating enzymes as editing enzymes. Here, we propose direct editing of N-glycosylated proteins using de-N-glycosylating enzymes to modify N-glycosylation and simultaneously alter the relevant asparagine residue to aspartate in living cells. Selective protein deglycosylation editors were developed by fusing high-affinity protein-targeting peptides with active peptide:N-glycanases (PNGases). Three crucial cell membrane proteins, PD-1, PD-L1, and severe acute respiratory syndrome coronavirus-2 (SARS-CoV-2) spike protein, were chosen to be tested as a proof of concept. N-linked glycans were removed, and the relevant sites were converted from Asn to Asp in living mammalian cells, destabilizing target proteins and accelerating their degradation. Further investigation focused on SARS-CoV-2 spike protein deglycosylation editing. The collaboration of LCB1-PNGase F (PNGF) effectively reduced syncytia formation, inhibited pseudovirus packaging, and significantly hindered virus entry into host cells, which provides insights for coronavirus disease 2019 (COVID-19) treatment. This tool enables editing protein sequences post-de-N-glycosylation in living human cells, shedding light on protein N-glycosylation functions, and Asn to Asp editing in organisms. It also offers the potential for developing protein degradation technologies.

KEYWORDS N-glycosylated proteins; peptide:N-glycanase (PNGase), protein-targeting peptides; deglycosylation; protein sequence editing; protein degradation

INTRODUCTION

The development of clustered regularly interspaced short palindrome repeats (CRISPR)/CRISPR-associated protein 9 (Cas9) technology since 2012 has triggered a revolution in the field of gene editing, bringing hope for the treatment of genetic diseases in humans [1,2]. Meanwhile, current research in protein modification studies primarily focuses on protein degradation methods, such as the widely popular proteolysis-targeting chimera (PROTAC) technology. This technology primarily aims at degrading an entire target protein through well-designed bifunctional molecules that consist of three key components: a ligand for the target protein, a ligand for an E3 ubiquitin ligase, and a linker connecting the two ligands [3]. Another approach to degrading a target protein involves the selective cleavage of proteases that Blum et al. developed [4]. This method includes reprogramming the specificity of proteases, through a phage-assisted evolution system with simultaneous positive and negative selection, to selectively cleave new targets of therapeutic interest [4].

Thus far, explorations into targeted protein editing techniques have just begun, but are still in their early stages. In 2021, Ge et al. developed a nanobody-fused split O-GlcNAcase (OGA) tool to selectively remove O-linked N-acetylglucosamine (O-GlcNAc) from several targeted O-glycosylated proteins, including the transcription factors like c-Jun and c-Fos [5]. Similarly, Pedram et al. designed a nanobody-fused StcE protease system for targeted degradation of cancer-associated mucins by recognizing and cleaving at the joint peptide and glycan motifs (S/T-X-S/T, where the first serine/threonine must bear an O-

glycan for cleavage to occur) [6]. These well-designed strategies focused on O-glycosylated proteins, utilizing de-O-glycosylating enzymes and specific proteases to edit and modify the targeted proteins without altering the amino acids in protein sequences. Ruvkun et al. have discovered the natural phenomenon of protein sequence editing and its significant roles in protein functions across eukaryotes since 2019 [7]. For instance, in *Caenorhabditis elegans* and *Homo sapiens*, deglycosylation-dependent 'sequence editing' of SKN-1A/Nrf1 by PNG-1/human PNG1 (NGLY1) leads to its nuclear localization and transcriptional activation of proteasome subunit genes [8]. These studies would induce an imagination for the development of precisely targeted protein editing techniques.

It is well-known that N-glycosylation refers to the attachment of polysaccharides to the free amino group of asparagine in the peptide chain of proteins, thereby assembling the sugar chains onto proteins [9]. N-glycosylation typically occurs at asparagine residues within the amino acid sequence motif Asn-X-Ser/Thr, where X can be any amino acid except proline. In eukaryotic cells, the majority of cell membrane glycoproteins undergo extensive N-linked glycosylation. This post-translational modification plays crucial roles in various biological functions, such as protein folding and stability, cell–cell communication, membrane protein trafficking, pathogen invasion, and immune response [10,11].

In this study, we proposed a selective de-N-glycosylation protein editing approach, which is capable of performing protein sequence editing in living cells by achieving N-glycan removal and amino acid conversion (Asn to Asp) simultaneously. As a proof of concept, three membrane proteins (programmed cell death protein-1 [PD-1], programmed cell death-1 ligand 1 [PD-L1], and severe acute respiratory syndrome coronavirus-2 [SARS-COV-2] spike) in which N-glycosylation plays a significant role in their function were selected as the target proteins for editing. It is widely recognized that PD-1, its ligand, and PD-L1, each possess four N-glycosylation sites. Accumulating evidence suggests that N-glycosylation modifications of PD-1 and PD-L1 play a significant role in maintaining their protein biosynthesis, stability, and interaction. Blocking any glycosylation site (N49, N58, N74, N116 on PD-1) would lead to decreased stability and expression levels of PD-1, suggesting a close correlation between PD-1 glycosylation and its stability and expression [12]. The glycosylation of N192, N200, and N219 on PD-L1 has been reported to create a steric hindrance effect, inhibiting PD-L1 degradation through the GSK3β-mediated 26S proteasome machinery, thus contributing to the stabilization of PD-L1 [13]. The inhibition of N-glycosylation of PD-1/PD-L1 leads to a reduction in their mutual interaction, thereby significantly enhancing the anti-tumor effect [14].

Apart from human-origin proteins, many membrane-bound proteins derived from pathogenic viruses, such as the SARS-CoV-2 spike protein and the H3N2 influenza A virus hemagglutinin (HA) protein, are also highly N-glycosylated. It has been confirmed that the SARS-CoV-2 spike protein contains 22 N-glycosylation sites [15], while the HA protein of the pandemic H3N2 A/Hong Kong/1/1968 contains 7 N-glycosylation sites [16]. In general, these N-glycosylation modifications assist in the proper folding and stabilization of the protein structure and facilitate the transport of the expressed protein within the infected host cell, as well as the budding of virus particles [10,17,18]. They also influence the interaction between the viral membrane proteins and their host cell receptors, which is critical for viral entry and subsequent replication. Moreover, acting as a "glycan shield," the N-glycans can also hide vulnerable epitopes on these proteins, making it more challenging for the immune system to recognize and attack the virus [18,19]. Additionally, the glycans on viral membrane proteins facilitate the binding of virus particles to the cell membrane by interacting with cell surface lectins as seen with SARS-CoV-2 [20].

Most studies on de-N-glycosylation have primarily focused on inhibiting the biosynthesis of N-glycosylation. This has been achieved through various techniques, including genetic modifications such as site-specific mutagenesis on DNA of decoding amino acid of Asn sites [21,22], knocking down or out genes involved in N-glycan generation and transfer (e.g., MGAT1, STT3A) [23,24], treatment with chemical inhibitors (e.g., tunicamycin, NGI-1) [25], using metabolic inhibitors such as 2-deoxyglucose *in vivo* [12], as well as enzymatic treatment *in vitro* (such as PNGase F or Endo H) [23]. However, technologies capable of generating naturally occurring deglycosylated forms at the protein-based amino acid level, involving the removal of N-glycans and the conversion of amino acid residues from Asn to Asp within living cells, have not yet been reported.

In this study, we report a protein sequence editing technique that allows for the selective editing of cell-surface glycoproteins in living cells directly at amino acid residues. This technique which relies on deglycosylation for targeted N-linked glycoproteins, has the potential to advance the investigation of specific N-glycan-associated functions and roles in protein sequence editing. It involves the combination of well-validated high-affinity protein-targeting peptides with various active peptide:N-glycanase (briefly referred to as PNGase or PNG1) sourced from different organisms including PNGase F from *Elizabethkingia miricola* and ScPNG1ΔH1 from *Saccharomyces cerevisiae*.

RESULTS

Design and Evaluation of Deglycosylation-dependent Protein Editors for Selected Transmembrane Glycoproteins

In the pursuit of developing effective protein editing tools, we designed multiple forms of protein editors, each consisting of three components: a targeting peptide, an editing enzyme, and a linker in between (Figure 1A). To begin, we employed three PNGase enzymes derived from different sources to create the initial protein editors (Figure 1B). They exhibit de-N-glycosylating enzyme functions despite large differences in protein sequences and functional domains among them [26]. PNGase F (PNGF), derived from *E. miricola,* is a commercially available enzyme that exhibits high activity and broad substrate specificity toward a wide range of glycoproteins and glycopeptides in both native and denatured forms [27]. Unlike prokaryotic PNGF, the various eukaryote-derived PNG1 enzymes were traditionally considered to primarily target misfolded or denatured N-linked glycoproteins [28]. However, deletion of the N-terminal H1 helix (Png1p-ΔH1, referred to as ScPNG1ΔH1 in this study) from yeast PNG1 enhances its N-glycanase activity toward denatured glycoproteins. Surprisingly,

it also shows high deglycosylation activity toward native glycoproteins [29]. Wu et al. recently discovered that NGLY1 (human PNG1) successfully recognizes and deglycosylates well-folded glycosylated PD-1 under the linkage of murine double minute 2 (MDM2) [30]. In addition, NGLY1 shares an 84% identity with mouse PNGase and they both possess the same functional domains, indicating their close similarity [26,31]. The truncated version of mouse PNG1 (mPng1-ΔC, amino acid 1–471) retained its PNGase activity, indicating that the N-terminal domain and the middle domain of mPng1p are important for PNGase activity [32]. In addition to testing PNGF and full-length NGLY1 as editing enzymes, a truncated ScPNG1ΔH1 lacking the N-terminal H1 helix and a truncated NGLY1(1–474) lacking the C-terminal domain were also evaluated in this study.

To produce active editing enzymes capable of being expressed in human cells, we removed the signal sequence (1–40 aa) of PNGF from *E. miricola*, and the N-terminal helix H1 (1–32 aa) of ScPNG1 from *S. cerevisiae*. Both enzymes were then subjected to human codon optimization. As a proof of concept, we targeted a subset of biologically significant glycoproteins localized to the cell membrane for editing. These targets included two endogenous human proteins associated with cancer diseases, PD-1 and PD-L1, and two exogenous viral proteins, the spike protein of SARS-CoV-2 and the HA protein of H3N2 influenza A virus (Figure S1). We then searched and gathered a limited number of published protein-targeting peptides with confirmed high affinity [33–36] (Table S1). Subsequently, we constructed dozens of editors in diverse forms by fusing certain peptides to three distinct PNGase enzymes *via* several widely used linkers, respectively (Figure 1C-1D, Table S2).

We next evaluated the efficacy of these editors by transiently transfecting the respective constructed plasmids into HEK293T cells or HEK293T stable cells expressing spike proteins. Firstly, it was evident that PNGF demonstrated high de-N-glycosylation activity toward PD-1, PD-L1, and the SARS-CoV-2 spike protein, while ScPNG1ΔH1 exhibited only moderate or low performance in removing N-linked glycans from these various glycoproteins (Figure 2A-2C). This outcome was expected due to the disparate optimal temperatures of PNGF and ScPNG1ΔH1 enzymes; PNGF functions optimally around 37 °C, whereas ScPNG1ΔH1 operates optimally at 30 °C. Moreover, PNGF has higher enzyme activity toward all kinds of denatured and native N-linked glycoproteins and glycopeptides and is capable of cleaving an entire glycan from a glycoprotein, including all three glycan types (high mannose, hybrid, and complex). In contrast, yeast PNG1 was reported to prefer glycoproteins containing high mannose over those bearing complex-type oligosaccharides [37]. As a result, optimization by combing various specific protein-binding peptides with PNGF or ScPNG1ΔH1 yielded diverse outcomes for different target proteins. For example, a small peptide named LCB1, well-designed by Cao et al. [38], was chosen in this study to target the full-length wild-type form or its uncleavable form of the SARS-CoV-2 spike protein. In this study, the wild-type form is named S-WT, while the uncleavable form is named S-Mutant with amino acids on sites 682–685 ('RRAR') mutated to 'GGSG'. The mass-shifted bands provided clear evidence that the resulting conjugate, termed LCB1-PNGF, achieved more extensive deglycosylation of the spike protein, even exhibiting lower expression levels compared with PNGF alone (Figure 2D-2E). Despite not being comparable to LCB1-PNGF, LCB1-ScPNG1ΔH1 exhibited higher efficacy in deglycosylating the full-length wild-type spike protein compared with ScPNG1ΔH1 alone (Figure 2F-2G). At last, we decided not to pursue further investigation with NGLY1 due to its lack of significant impact on PD-1/PD-L1, even when fused with specific protein-targeting peptides (Figure 2A-2B).

As deglycosylation-dependent protein modifications were successfully performed on the spike protein of SARS-CoV-2, we further conducted a co-immunoprecipitation (co-IP) assay and confirmed the protein–protein interaction between the engineered editors (PNGF and LCB1-PNGF) and the targeted spike protein (Figure 2H-2I). Additionally, we utilized immunofluorescence confocal microscopy to observe the co-localization of LCB1-PNGF with the spike protein (Figure 2J). Subsequently, the specific deglycosylated and deamidated sites of the spike protein, generated by the two editors, were precisely verified through immunoprecipitation enrichment and liquid chromatography-mass spectrometry (LC-MS) analysis. Concerned with the fact that the wild-type full-length spike protein (S-WT) is easily cleaved into S1 and S2 subunits at the furin cleavage site (^{682}RRAR^{685}) by host proteases, we established a stable HEK293T S-Mutant cell line expressing a mutated spike protein that hinders protein cleavage by substituting 'RRAR' with 'GGSG'. This modification aimed to enrich a sufficient amount of full-length spike protein through immunoprecipitation [39]. The LC-MS analysis successfully detected and statistically collected specific deglycosylation-dependent deamidated sites (Asn to Asp) among the S-Mutant samples. Consistent with the immunoblotting results, more deamidated sites were observed in samples treated with LCB1-PNGF (∼15 deamidated sites) than in PNGF-treated samples (∼11 deamidated sites) (Figure 2K, and Supplementary Materials Word and Excel 1–4).

We observed clear evidence that the fusion of a peptide to the enzyme achieved more extensive deglycosylation and lower expression levels of the spike protein, exemplified by LCB1-PNGF compared with PNGF alone (Figure 2E-2H). This phenomenon indicates that although the fusion of the LCB1 peptide might have compromised the expression of PNGF, their combination likely enhances the delivery of the enzyme to the spike protein. Consequently, the resulting increased local concentration of the peptide-enzyme fusion led to more extensive deglycosylation and instability of the target protein. However, we acknowledge that not all fusions have proven effective. Despite multiple attempts, including the use of different antibodies for detection, we were unable to observe deglycosylated forms of H3N2-HA (Figure S2A). In contrast to the effective performance of LCB1-PNGF on the spike protein, the fusion of a peptide to PNGF for targeting PD-1 or PD-L1 did not outperform PNGF alone (Figure S2B-S2G). We hypothesize that the fusion of specific small peptides might have damaged the proper folding and assembly of the PNGF protein, potentially compromising its enzyme activity toward PD-1 and PD-L1. Alternatively, the high enzyme activity of PNGF may have interfered with the substrate selectivity of protein-targeting peptides. Future optimization of these peptide-PNGF editors will be necessary for their

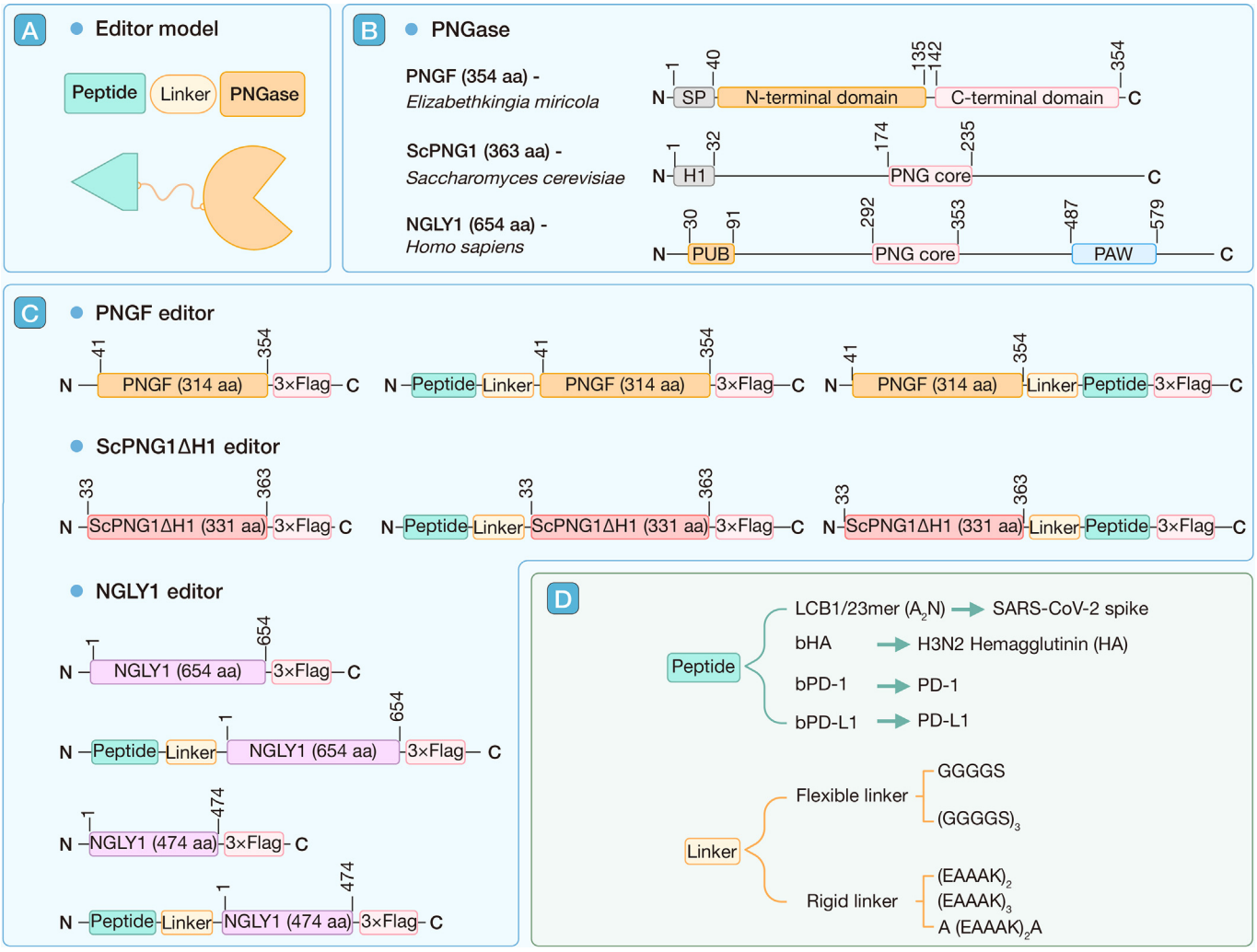

Figure 1. Design and development of deglycosylation-dependent protein editors
(A) A simplified schematic diagram of the constructed protein deglycosylation sequence editing tool. (B) Three different species-derived peptide:N-glycosidases. (C) Various arrangements of the constructed protein editors, including a protein-targeting peptide, an active PNGase (PNGF lacking signal peptide sequence, ScPNG1 lacking H1 [ScPNG1ΔH1], a full-length NGLY1 and its truncated version NGLY1[1–474]), and a linker for connection. A 3×Flag tag was attached to the C-terminus of the protein editor for subsequent detection of protein expression. (D) The display of high-affinity peptides used for targeting PD-1, PD-L1, and the spike protein of SARS-CoV-2, as well as different forms of flexible or rigid linkers utilized in this study. Abbreviations: PNGase, peptide:N-glycanase; PNGF, PNGase F; ScPNG1, *Saccharomyces cerevisiae* peptide:N-glycanase; NGLY1, human PNG1; PD-1, programmed cell death protein-1; PD-L1, programmed cell death-1 ligand 1; SARS-CoV-2, severe acute respiratory syndrome coronavirus-2.

application to PD-1, PD-L1, and other glycoproteins of interest. However, a collaboration between ScPNG1ΔH1 and peptide bPD-1 or bPD-L1 fused to either its N-terminal or C-terminal orientation resulted in relatively higher levels of deglycosylated PD-1/PD-L1 protein than ScPNG1ΔH1 alone (Figure S2B-S2G). This is likely due to the fusion of the peptide to the relatively low-activity ScPNG1ΔH1, which improved substrate selectivity toward the target proteins. Therefore, future studies should focus on optimizing and establishing effective fusions between suitable peptides and active PNGase with appropriate enzyme activities, linked by suitable linekers, for diverse target proteins.

The Optimized Editors Disrupt the Stability and Accelerate the Degradation of Targeted Glycoproteins

It has been well-established that N-glycosylation plays a crucial role in maintaining protein stability, while deglycosylated proteins usually degrade rapidly through the endoplasmic reticulum-associated degradation (ERAD) process. As depicted in Figure 2, we observed that the editors could decrease the expression levels of the target proteins. To validate this observation and investigate turnover rates of the target proteins following editing by our editors, we employed cycloheximide (CHX) treatment, a well-established method to inhibit *de novo* protein synthesis. CHX acts by blocking ribosomal translocation during translation, thereby allowing us to assess the degradation kinetics of PD-1, PD-L1, and the spike protein without new protein synthesis. Upon the addition of 100 μM CHX to reach a final concentration, the protein levels of PD-1, PD-L1, and the SARS-CoV-2 spike protein were monitored over time using immunoblotting. As previously mentioned, although the two conjugates, bPD-1-PNGF and bPD-L1-PNGF, were not able to achieve the same level of deglycosylation as PNGF alone when targeting

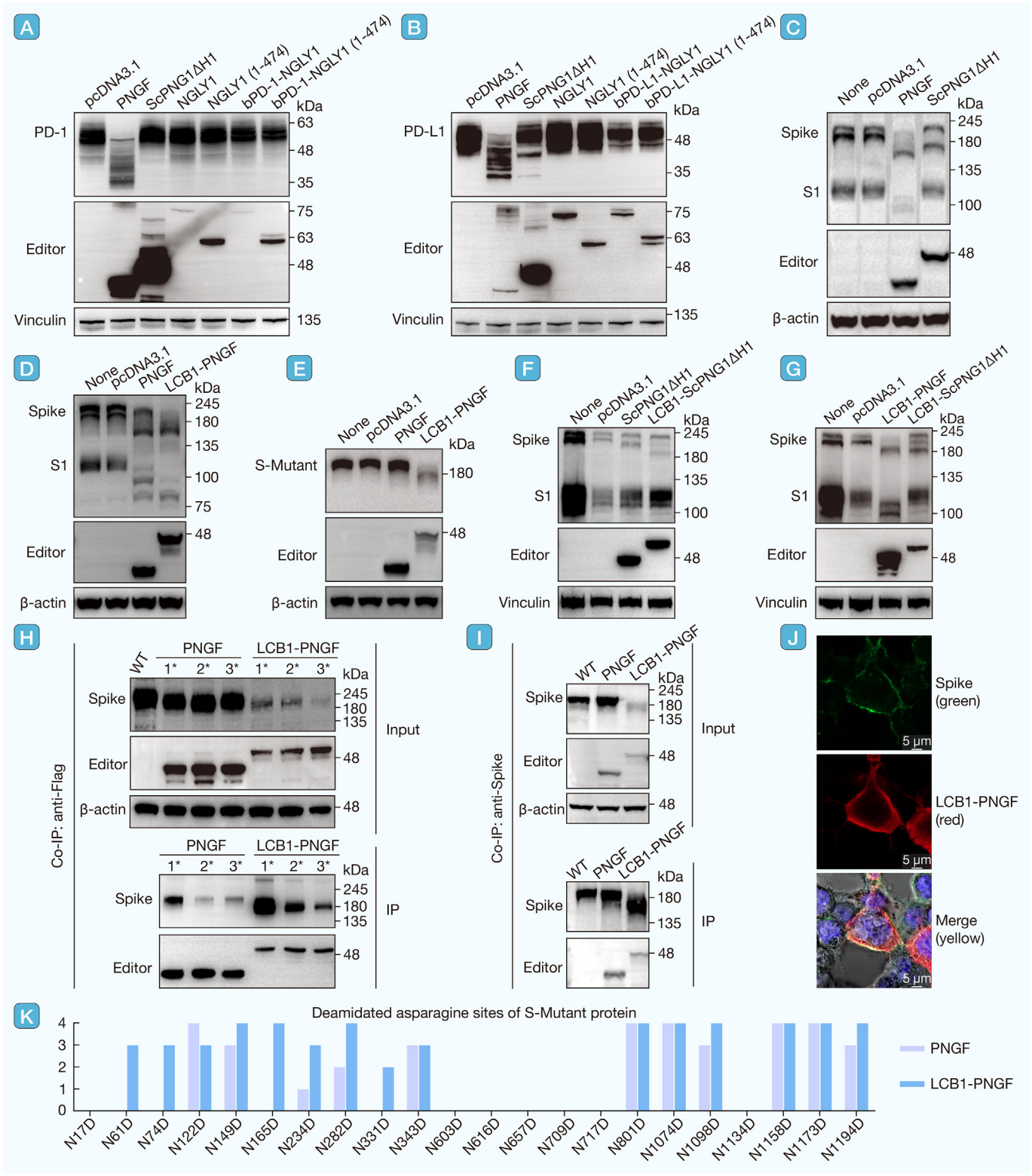

Figure 2. The constructed and optimized protein editors efficiently removed N-linked glycans from PD-1, PD-L1, and SARS-CoV-2 spike protein

(A-C) The effects of three different peptide:N-glycanases on target protein PD-1, PD-L1, and the SARS-CoV-2 spike protein were analyzed. PNGF exhibited a high de-N-glycosylation activity toward PD-1, PD-L1, and SARS-CoV-2 spike protein, whereas ScPNG1ΔH1 only showed a moderate or rather low performance on removing N-linked glycans from these different glycoproteins. There was no noticeable impact of a full-length or truncated version of NGLY1 on PD-1/PD-L1 even when fused with specific protein-targeting peptides. (D–E) LCB1-PNGF induced more extensive deglycosylation toward both wild-type (S-WT) and mutated spike protein (S-Mutant, 682'RRAR'685 mutated to 'GGSG'), even though it exhibited lower expression levels compared with PNGF alone. (F–G) Despite not being comparable to LCB1-PNGF, LCB1-ScPNG1ΔH1 exhibited higher efficacy in deglycosylating the full-length wild-type spike protein, when compared with ScPNG1ΔH1 alone. (H–I) Co-immunoprecipitation experiment confirmed the protein–protein interaction between the constructed editors (PNGF-3×Flag and LCB1-PNGF-3×Flag) and the targeted

(legend continued on next page)

PD-1 and PD-L1, respectively, they both expedited the protein degradation process. As shown in Figure 3A, PD-1 exhibited a faster degradation rate when treated with bPD-1-PNGF than PNGF alone over 12 h after CHX addition. Similar trends were observed for PD-L1 and the spike protein (Figure 3B-3C). However, although LCB1-ScPNG1ΔH1 demonstrated good performance in deglycosylation of the spike protein, it did not exhibit obvious superior efficiency in destabilizing the full-length spike protein and its S1 subunit when compared with either the empty vector or ScPNG1ΔH1 alone (Figure 3D).

Given the effective deglycosylation and destabilization of the spike protein by LCB1-PNGF, we employed flow cytometric analysis to precisely quantify the total concentrations of spike protein in HEK293T cells after treatment with either PNGF or LCB1-PNGF. The experiment was conducted by co-transfecting HEK293T cells with a plasmid expressing the S-WT-EGFP (enhanced green fluorescent protein) protein and a plasmid expressing the respective editor. The active editors included PNGF and LCB1-PNGF, while an empty vector (pcDNA3.1) and an inactive mutant PNGF(D60N) were used as negative controls. After 48 h post-transfection, cells were collected to measure the mean fluorescence intensity of EGFP using flow cytometry. The results revealed that LCB1-PNGF induced a 50% reduction in protein levels relative to the control cells transfected with the empty vector pcDNA3.1, while cells expressed with PNGF alone only led to a nearly 20% reduction (Figure 3E). These findings implied the combined efforts of an active PNGF and an appropriate protein-targeting peptide were necessary to achieve such remarkable degradation of the targeted glycoproteins.

Furthermore, upon treatment with MG132 (a proteasome inhibitor) or NH_4Cl (an autophagy inhibitor) in HEK293T cells stably expressing the S1 subunit, we confirmed that the deglycosylated form of the spike S1 subunit primarily undergoes the ERAD pathway *via* the proteasome rather than the autophagy pathway. This was evidenced by the result that treatment with MG132 led to the apparent restoration of higher levels of deglycosylated S1 subunit in LCB1-PNGF samples (Figure 3G-3H). Additionally, MG132 treatment resulted in a more pronounced restoration of the full-length S-WT protein in the LCB1-PNGF sample compared with the PNGF sample and three negative controls (Figure 3F). This inversely illustrates an increase in degradation of the spike protein following LCB1-PNGF editing, a trend that was consistently observed in Figure 3G as well. Taken together, these approaches provided compelling evidence that deglycosylation-dependent protein sequence editing, especially when performed by PNGF-related editors fused with proper targeting peptides, resulted in accelerated degradation and a subsequent significant decrease in the intracellular concentrations of the diverse targeted glycoproteins.

De-N-glycosylation of SARS-CoV-2 Spike Proteins Disrupts Cell–Cell Fusion and Impairs Virus Entry into Host Cells

There have been consistent reports highlighting the crucial role of N-glycosylation in the spike protein of SARS-CoV-2 for the virus's entry into host cells. It is well established that the interaction between the receptor-binding domain (RBD) of the spike protein and angiotensin-converting enzyme 2 (ACE2) is pivotal for SARS-CoV-2 entry into host cells. LCB1, a high-affinity mini-protein designed by Cao et al., binds to the RBD of the spike protein effectively, competes with ACE2, and efficiently inhibits SARS-CoV-2 infection of cells [38]. Expanding on our observation that LCB1-PNGF effectively facilitated the deglycosylation and degradation of the spike protein, we further investigated the impact of this fusion editor on cell–cell fusion between spike-expressing cells and ACE2-expressing cells.

To evaluate the effect of deglycosylation-mediated protein editing on cell–cell fusion and syncytia formation mainly induced by the spike protein, we conducted a previously described luciferase-based quantification assay. This assay allowed us to accurately measure the inhibitory efficiency of all the editing agents developed for the spike protein [40]. The results indicate that when the LCB1 peptide is either fused to PNGF or ScPNG1ΔH1, the resulting conjugates demonstrated greater effectiveness in blocking cell–cell fusion between HEK293T-spike-expressing cells and HEK293T-ACE2 expressing cells, compared with another computationally optimized peptide 23mer (A_2N) (Figure S3A-S3B). Subsequently, three combinations of LCB1 and PNGF, with either a flexible (GGGGS) or rigid (EAAAK) linker in between, were investigated to identify the optimal combination. Finally, the most pronounced reduction (around 80%) of syncytia formation was observed with LCB-PNGF treatment (Figure 4A). In line with the obtained results, we conducted a visual experiment by mixing HEK293T spike-EGFP co-expressing cells, which were pretreated with different editors (PNGF and LCB1-PNGF), with HEK293T-ACE2 expressing cells, while empty vector and inactive mutant PNGF(D60N) were used as two negative controls. Fluorescence microscopy revealed that the pretreatment with LCB1-PNGF significantly inhibited cell–cell fusion, leading to minimal syncytia formation between the two cells (Figure 4B).

As the optimal candidate in our study, LCB1-PNGF was selected to further assess its effectiveness in inhibiting pseudovirus production and virus entry into host cells (Figure 4C). As shown in Figure 4D, the spike protein on the pseudovirus surface, pretreated with LCB1-PNGF, displayed a reduced protein level due to increased deglycosylation, contrasting the control with pcDNA3.1 empty vector. As a result, the pseudovirus lost its viral infection ability by more than 80% when infecting all three popular host cells, including HEK293T, Calu-3, and PC-9 cells

spike protein. (J) LCB1-PNGF (red) co-localized with the spike protein (green) observed by immunofluorescence laser confocal microscopy. (K) Specific deglycosylation-dependent deamidated sites (Asn to Asp) among S-Mutant samples induced by PNGF or LCB1-PNGF editor were detected by LC-MS analysis and statistically collected with four biological replicate experiments. Consistent with the immunoblotting results, more deamidated sites were observed in LCB1-PNGF samples (15 deamidated sites) than in PNGF samples (11 deamidated sites).

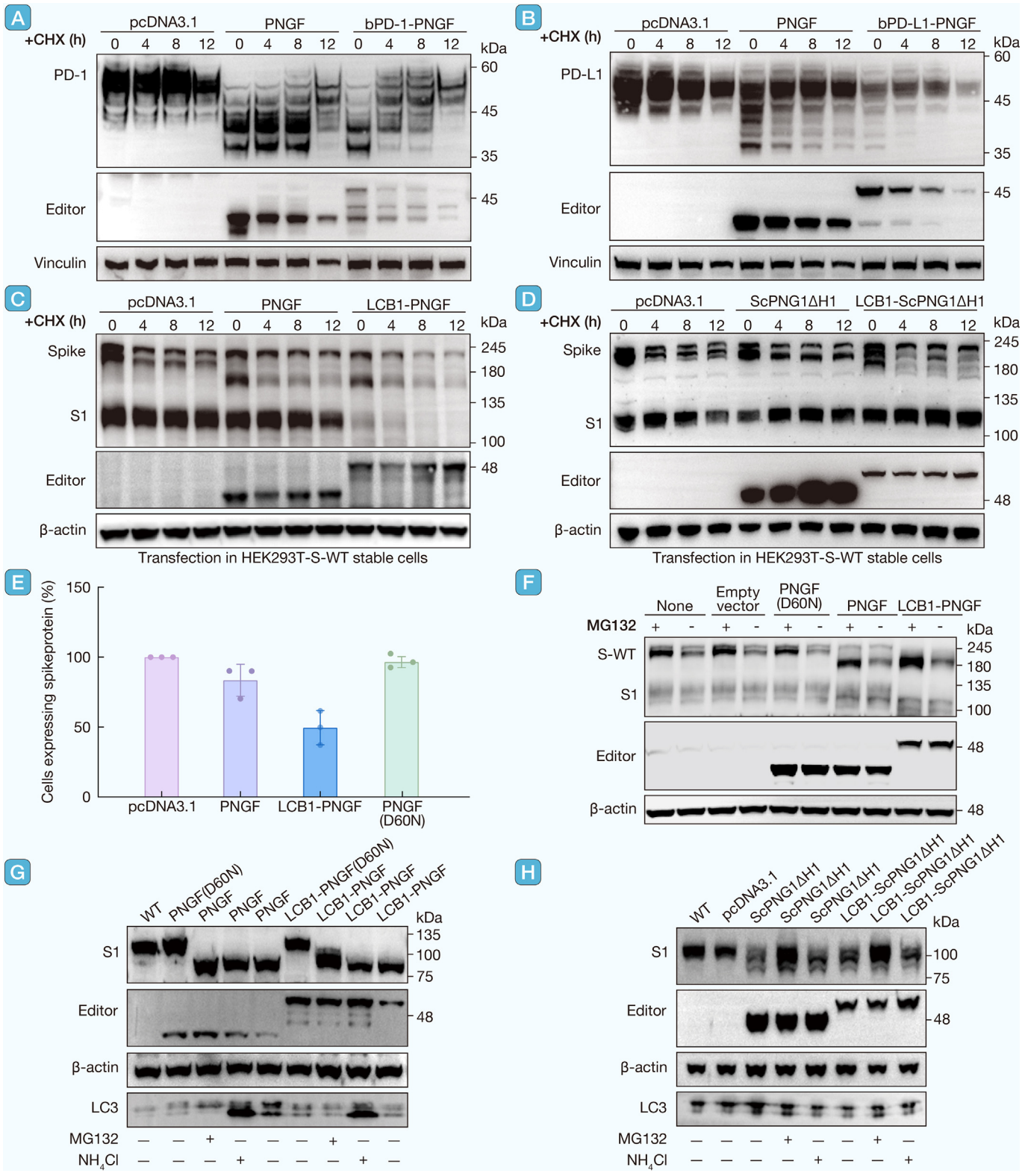

Figure 3. The optimized editors disrupt protein stability and accelerate the degradation process of targeted glycoproteins
(A-D) Cycloheximide treatment experiments confirmed that bPD-1-PNGF, bPD-L1-PNGF, and LCB1-PNGF accelerated the degradation process for PD-1, PD-L1, and the spike protein, respectively, compared with PNGF alone. (E) Flow cytometry analysis indicated that LCB1-PNGF induced a ~50% reduction of spike protein levels relative to the empty vector pcDNA3.1 while PNGF alone only led to less than 20% reduction of spike protein levels by measuring EGFP mean fluorescence intensity. (F–H) MG132 treatment experiment proved that the de-glycosylated forms of the full-length wild-type spike protein and its S1 subunit caused by different editors primarily undergo the ERAD pathway *via* the proteasome, rather than the autophagy pathway. Abbreviations: EGFP, enhanced green fluorescent protein; ERAD, endoplasmic reticulum-associated degradation.

(Figure 4E-4G). Then a CellTiter-Glo® Luminescent Cell Viability assay was employed to reveal that the appropriate amounts of various optimized editors including LCB1-PNGF used in our experiments for an incubation time of 48h were not toxic to cells (Figure S3C).

Based on our experimental LC-MS data characterizing the actual editing sites and the availability of the 3D structure of the SARS-CoV-2 spike protein (PDB ID: 6XR8), we conducted a mapping of the deglycosylated and glycosylated sites onto the 3D structure of the spike protein (Figure S3D, the N74, N1173, and N1198 sites were unlabeled due to their absence in the available 3D structure). This mapping was performed for samples treated with PNGF or LCB1-PNGF, respectively. The LCB1-PNGF conjugate led to the editing of four additional sites compared with PNGF alone, namely N61, N74, N165, and N331. Among them, the N61Q mutation was found to decrease spike protein expression and hinder its incorporation into spike-pseudotyped lentivirus, subsequently impairing entry into cells expressing the ACE2 receptor [22]. N-glycans at site N165 are crucial for modulating the spike's receptor-binding domain (RBD) dynamics, which is essential for ACE2 recognition [41]. N331, situated within the RBD of the S1 subunit, is also crucial; its deglycosylation significantly weakens the RBD's affinity for ACE2 [42]. Collectively, these three glycosylated sites are vital for pseudovirus assembly and entry into ACE2-expressing cells. Consequently, compared with PNGF alone, LCB1-PNGF-mediated editing leads to a more substantial decrease in cell–cell fusion and a greater reduction in pseudoviral infection.

DISCUSSION

Herein, we report a deglycosylation-dependent protein sequence editing tool to selectively remove N-glycans and simultaneously convert glycosylated asparagine (Asn) residues to aspartate (Asp) of the desired cell membrane glycoproteins in living cells. In particular, we demonstrate that the carefully constructed and optimized PNGF-related and ScPNG1ΔH1-related editors achieved varying degrees of deglycosylation toward PD-1, PD-L1, and SARS-CoV-2 spike proteins, except for H3N2 HA protein. However, NGLY1, which is essential for de-N-glycosylation in human cells, has not been found functional for targeting these proteins in our work. This suggests that these editors may have some specific preferences, which hinder their effectiveness on all types of N-linked glycoproteins. Among the three PNGase enzymes utilized in this study, PNGF, exhibiting high enzyme activity, effectively catalyzed deglycosylation of PD-1, PD-L1, and the SARS-CoV-2 spike proteins. In contrast, ScPNG1ΔH1 demonstrated only moderate to low performance in this regard. Notably, the LCB1-PNGF conjugate enhanced substrate selectivity, specifically targeting the spike protein, facilitating more profound protein deglycosylation, and significantly reducing cell–cell fusion and viral entry into host cells.

Deglycosylation caused by these editors led to a more rapid degradation rate through the ERAD process *via* the proteasome. Several studies have highlighted specific N-glycosylation sites critical for the spike protein's stability and proper folding. For example, it has been reported that N-glycans at positions N165, N234, and N343 of the SARS-CoV-2 S protein stabilize the RBD in an open state and thus contribute to an increase in infectivity [43–45]. Removal of N-glycans in N1074 reduced the stability of the SARS-CoV-2 spike protein, indicating that N-linked glycosylation at residue N1074 is crucial for the stability of the spike protein [46]. Tian et al. have revealed an intriguing "O follow N" pattern in the SARS-CoV-2 spike protein [47]. Their research highlights that O-glycosylation tends to occur near the N-glycosylation sequence. Specifically, they identified seven O-glycosylation modification sites situated on Ser/Thr residues of the NXS/T motif. Moreover, they observed that the N616Q mutation effectively eliminates O-glycosylation at T618, suggesting that the presence of N-glycosylated Asn is necessary for O-glycosylation at the T618 site. It is widely acknowledged that O-glycans play a crucial role in protein stability and function. In light of this, our tools target the removal of N-glycans from target proteins, which may also impact other protein post-translational modifications, such as O-glycosylation and phosphorylation at adjacent sites. Based on the findings of these studies, our deglycosylation editing tools facilitate the destabilization of target proteins, leading to their rapid degradation through the proteasome pathway. LC-MS analysis revealed that several E3 ubiquitin-protein ligases were frequently detected in the immunoprecipitation samples. The most commonly observed ligases with the highest levels were HUWE1 and CHIP (also known as STUB1) (listed in Supplementary Material Excel 5). Additionally, other ligases such as RBBP6, UHRF1, UBR4, UBR5, HECTD1, RBX1, and ARIH1 were also found with significant frequency. This suggests that these E3 ubiquitin-protein ligases probably made a major contribution in facilitating the degradation of deglycosylated spike protein through subsequent ubiquitination and ERAD process.

Our study highlights the efficacy of targeted de-N-glycosylation in promoting natural protein degradation *via* the proteasome, akin to findings observed in recent studies involving targeted de-O-glycosylation [5] and dephosphorylation [48]. In contrast to PROTAC technology, which relies on small molecules to degrade specific target proteins within cells, our approach simplifies the process by facilitating natural protein degradation without the need for screening E3 ligases. This bypasses the challenges associated with PROTAC design, including the requirement for bifunctional molecules and suitable E3 ligases for each target protein. Our deglycosylation editing tools offer a straightforward yet potent alternative for modulating protein levels within cells. Additionally, our de-N-glycosylation tool primarily targets N-glycosylated proteins on the cell membrane, distinguishing it from the nanobody-fused split OGA tool that focuses on nucleocytoplasmic proteins, particularly transcription factors. While our approach effectively edits N-glycosylated proteins on the cell membrane, its applicability to other protein types or subcellular locations may be limited. Nonetheless, considering the significant involvement of high or abnormal N-glycosylated proteins in diseases like infections and cancers, our tool introduces innovative strategies for manipulating glycans within cells.

SARS-CoV-2 spike protein plays a critical role in virus binding to infected cells and facilitating virus invasion through interacting with host receptor ACE2. Removing N-glycans by optimized LCB1-PNGF conjugate led to a sharp reduction in spike protein

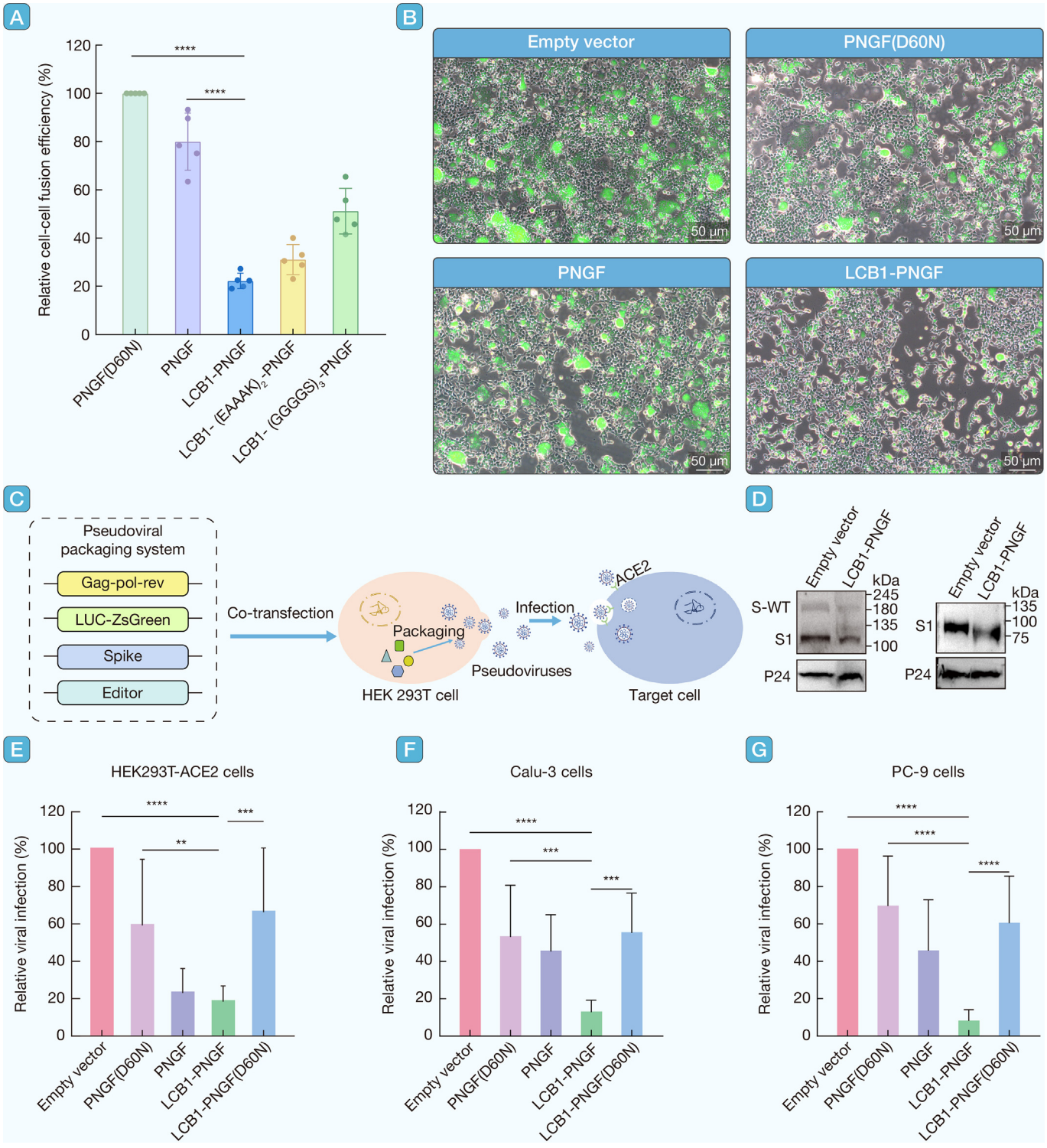

Figure 4. De-N-glycosylation of SARS-CoV-2 spike proteins disrupted cell–cell fusion and impaired virus entry into host cells
(A) A modified luciferase-based quantification assay demonstrated that deglycosylation protein editing of spike protein conducted by LCB1-PNGF editor resulted in the most pronounced reduction (~80%) of cell–cell fusion. (B) HEK293T spike-EGFP co-expressing cells were pre-treated by different editors (empty vector and inactive mutant PNGF(D60N) as two negative controls, PNGF and LCB1-PNGF). After 48 h post-transfection, they were collected and mixed with HEK293T-hACE2 expressing cells at a ratio of 1:1. After additional 24 h of incubation, images of syncytia formation were captured using a fluorescence microscope. It clearly showed that LCB1-PNGF pretreatment of spike protein led to a very low syncytia formation between the two cells, in line with the greatly reduced cell–cell fusion efficiency. (C) A schematic representation of SARS-CoV-2 pseudovirus production and virus entry into target cells. (D) The spike protein on the pseudovirus surface, pretreated with LCB1-PNGF editor, exhibited a lower protein level following deglycosylation, compared with the pcDNA3.1 empty vector. (E–G) The pseudovirus pretreated with LCB-PNGF editor lost its viral infection ability by more than 80% when infecting all three popular host cells, including HEK293T, Calu-3, and PC-9 cells. *$P < 0.05$, **$P < 0.01$, ***$P < 0.001$, and ****$P < 0.0001$.

level and significantly hindered pseudovirus production as well as virus entry into host cells. It was revealed by immunopeptidomic analysis that the deamidated HLA-bound peptides primarily originate from deglycosylated precursor proteins mediated by NGLY1/PNG1 during the ERAD process [49]. Ruvkun et al. suggested that protein deglycosylation and Asn to Asp editing not only serve as prerequisites for protein degradation *via* the proteasome but also potentially play a significant role in the immune system since processing peptides is a critical step in the immune presentation of both host and viral peptides [7]. These peptides may robustly activate T-cell cytotoxicity or B-cell maturation to mediate a stronger immune response against viral infections. Taken together, deglycosylation and Asn to Asp editing by our carefully optimized editors perhaps provide an alternative strategy for COVID-19 treatment and antiviral therapy.

We admit that there are notable limitations to our current peptide-enzyme conjugates for the deglycosylation and deamidation system. For instance, it is noteworthy that LCB1-PNGF continues to exhibit obvious off-target efficiency due to its high enzyme activity according to LC-MS analysis. Future studies should prioritize enhancing the balance between off-target rate and on-target efficacy in our protein editing technique. Genetic engineering approaches or chemical modifications could achieve this goal. Specifically, we propose exploring genetic engineering approaches to fine-tune the enzyme's properties, mainly involving site-directed mutagenesis to modulate the catalytic activity of PNGF. For example, point mutations such as T101A have been shown to halve enzyme activity, while D102N leads to a 70% decline, and Y85F retains only 10% activity [50]. Rational design and engineering combined with directed evolution hold promise for improving the thermostability and enzyme activity of ScPNG1ΔH1 and modifying NGLY1 for its utility in this technique. In the meantime, selecting high-affinity protein-targeting peptides or specific nanobodies may enhance on-target efficacy in future studies. We hope, in the future, to employ these approaches or modifications to provide precise control over enzyme activity, enabling customized editing of target proteins while minimizing off-target effects.

In conclusion, we present here an unconventional approach for targeted protein editing, focusing on the de-N-glycosylation of disease-associated proteins using a peptide-PNGase fusion editor. This system brings hope in uncovering the underlying mechanisms of their N-glycosylation modifications and the natural phenomenon of Asn to Asp protein sequence editing within living organisms in the future. Furthermore, this protein sequence editor provides an opportunity to open a new era of precise editing in living cells.

MATERIALS AND METHODS

Plasmids

The genes encoding PNGF (UniProtKB: P21163), ScPNG1ΔH1 (UniProtKB: Q02890), and NGLY1 (UniProtKB: Q96IV0) were human codon-optimized and synthesized by GENEWIZ (Jiangsu, China). They were then cloned into the pcDNA3.1 vector and fused with a C-terminal 3×Flag tag. Inactive mutants of PNGF(D60N) and ScPNG1ΔH1(D204A) were generated through site-specific mutagenesis using PCR. The gene fragments of protein-targeting peptides for PD-1 (UniProtKB: Q15116), PD-L1 (UniProtKB: Q9NZQ7), influenza A virus (strain A/Hong Kong/1/1968 H3N2) HA (UniProtKB: Q91MA7), and SARS-CoV-2 spike protein (UniProtKB: P0DTC2), which are listed in Table S1, were also synthesized by GENEWIZ. They were cloned into the PNGF, ScPNG1ΔH1, or NGLY1 plasmids in two different fusion orientations *via* a flexible or rigid linker in between to generate the required deglycosylation-dependent protein editors, as shown in Table S2. The genes encoding PD-1, PD-L1, H3N2-HA, and SARS-CoV-2 S-WT-Δ19 were synthesized by GENEWIZ and cloned into the pcDNA3.1 vector individually. Each gene, either encoding the full-length wild-type spike protein of SARS-CoV-2, or its spike-mutant form where the amino acids 'RRAR' at sites 682–685 were mutated into 'GGSG', or its S1 subunit fragment, was synthesized into the lentiviral expression vector pCDH which harbors the EGFP and puromycin gene sequence to generate HEK293T-S-WT, HEK293T-S-Mutant, or HEK293T-S1 stable cell lines through lentiviral infection.

Generation of Stable Cell Lines

To generate S-WT, S-mutant, and S1 stably expressing cell lines, HEK293T cells were co-transfected with the constructed pCDH vectors containing each gene encoding either S-WT-T2A-EGFP or S-Mutant-T2A-EGFP or S1-T2A-EGFP, psPAX2, and VSV-G plasmids *via* Lipo8000™ transfection reagent (Beyotime, Shanghai, China) to produce lentivirus containing either S-WT or S-Mutant or S1 transgene, respectively. After 72 h post-transfection, the lentivirus supernatant was harvested, filtered by using a 0.45 μm filter (MilliporeSigma, Hessian, Germany), and concentrated by using a Amicon® Ultra-15 Centrifugal Filter-100 kDa (MilliporeSigma, Hessian, Germany), and then transduced into HEK293T cells with 10 μg/mL polybrene (Beyotime, Shanghai, China). Finally, all three stable cell lines were EGFP-positive sorted by flow cytometry and maintained in selection using 2 μg/mL puromycin (Beyotime, Shanghai, China).

Cell Cultures and Plasmids Transfection

HEK293T cells were cultured in DMEM (Dulbecco's modified Eagle medium) (TransGen Biotech, Beijing, China) supplemented with 10% (*v/v*) fetal bovine serum (FBS) (TransGen Biotech, Beijing, China), along with 1% penicillin-streptomycin liquid (100×) (Solarbio, Beijing, China). HEK293T-S-WT, HEK293T-S-mutant, and HEK293T-S1 stable cells were cultured with the addition of 2 μg/mL puromycin (Beyotime, Shanghai, China). HEK293T-hACE2 stable cells were cultured with the addition of 100 μg/mL hygromycin B (PhytoTech Labs, Kansas, USA). Calu-3 cells were cultured in minimum essential medium (MEM, Solarbio, Beijing, China) with 10% FBS along with 1% penicillin-streptomycin liquid (100×). PC-9 cells were cultured in Roswell Park Memorial Institute (RPMI) Medium 1640 (Solarbio, Beijing, China) with 10% FBS. The cells were maintained at 37 °C with a 5% CO_2 concentration. Plasmid transfection was performed when the cells reached approximately 70%–80% confluence, following the instructions provided by the Lipo8000™ transfection reagent manufacturer. After 48 h post-transfection, the cells were harvested for further analysis.

In vivo Deglycosylation Assay

The appropriate amounts of constructed plasmids were transiently transfected into HEK293T cells or the respective stable cell lines using Lipo8000™ transfection reagent. After 48 h of cultivation, the cells were collected and lysed with RIPA lysis buffer (Solarbio, Beijing, China). Protein concentrations were quantified using the Pierce BCA Protein Assay Kit (Thermo Fisher Scientific, Massachusetts, USA). A total of 30 μg of protein was mixed with SDS-PAGE Sample Loading Buffer (ABclonal, Hubei, China) and heated at 100 °C for 5–10 min. The mixture was then separated on SurePAGE, Bis-Tris 4%–12% gels (GenScript, Jiangsu, China), and transferred onto a polyvinylidene fluoride (PVDF) transfer membrane (Thermo Fisher Scientific, Massachusetts, USA) using the eBlotTM L1 system (GenScript, Jiangsu, China). Protein expression levels of various editors constructed in this study were detected using anti-Flag antibody, and the deglycosylation effects on target proteins were investigated using their respective antibodies such as anti-PD-1 antibody, anti-PD-L1 antibody, anti-H3N2-HA antibody, and anti-SARS-CoV-2 spike antibody listed in Table 1.

Co-IP Assay and LC-MS Analysis

The appropriate amounts of the two constructed plasmids, pcDNA3.1-PNGF-3×Flag and pcDNA3.1-LCB1-PNGF-3×Flag, were transiently transfected into HEK293T-S-Mutant stable cells, respectively. After 48 h of cultivation, the cells were lysed using NP40 buffer for 15 min on ice. The supernatant was collected after centrifugation at 15,000 rpm for 5 min at 4 °C. Protein concentrations were quantified using the Pierce BCA Protein Assay Kit. Following the manufacturer's instruction, a Flag-tag Protein IP Assay Kit with Magnetic Beads (Beyotime, Shanghai, China) was employed to enrich proteins with Flag-tag and their interacting proteins. Similarly, the Anti-SARS-CoV-2 spike S1-NTD Magnetic Beads Immunoprecipitation (IP) Kit (Sino Biological, Beijing, China) was utilized to enrich spike proteins and their interacting proteins. Immunoblotting analysis was then conducted to confirm the protein expression levels of PNGF or LCB1-PNGF and the deglycosylation states of the spike-mutant (S-Mutant). Finally, the bands of enriched S-Mutant proteins were analyzed through LC-MS analysis to detect deaminated sites after deglycosylation induced by PNGF or LCB1-PNGF.

Immunofluorescence Assay

HEK293T-S-EGFP stable cells were transiently transfected with the appropriate amount of LCB1-PNGF plasmid in a 20 mm confocal dish (NEST, Jiangsu, China). After 48 h of cultivation, cells were fixed with 4% paraformaldehyde (Solarbio, Beijing, China) for 30 min at room temperature (RT). Following three washes with 1× PBS, cells were permeabilized with 0.1% Triton X-100 (Solarbio, Beijing, China) for 10 min at RT to allow antibody penetration. After another three washes with 1× PBS, cells were blocked with immunofluorescence blocking buffer (Beyotime, Shanghai, China) for 40 min at RT. Subsequently, cells were incubated with anti-Flag antibody (1:200) overnight at 4 °C, followed by ABflo 647-conjugated goat anti-rabbit IgG (H + L) (1:500) (ABclonal, Hubei, China) for 40 min at RT. After washing with 1× PBS three times, an antifade mounting medium with 4',6-diamidino-2-phenylindole (DAPI) (Beyotime, Shanghai, China) was applied to the cells for 5 min in the dark. Images were acquired using a Zeiss laser confocal microscope (LSM 900 with Airyscan 2, Zeiss, Baden-Wurttemberg, Germany).

Protein Degradation Assay

Cycloheximide Treatment

HEK293T cells were transiently co-transfected with the indicated plasmids, such as the PD-1 expressing plasmid and its deglycosylation editor (PNGF or bPD-1-PNGF), the PD-L1 expressing plasmid and its deglycosylation editor (PNGF or bPD-L1-PNGF), with an empty vector pcDNA3.1 as the negative control. Similarly, HEK293T-S-WT stable cells were transiently transfected with individual editor plasmids (PNGF, LCB1-PNGF, ScPNG1ΔH1, or LCB1-ScPNG1ΔH1). After 30 h of transfection, cells were incubated with 100 μM CHX (Aladdin, Shanghai, China) for up to 12 h. At the indicated time points, cells were collected and lysed with RIPA lysis buffer. Protein expression levels of editors and deglycosylation and degradation states of targeted proteins were determined by western blotting. Vinculin and β-actin were used as internal loading controls.

MG132 Treatment

HEK293T-S-WT stable cells were transiently transfected with the indicated individual plasmid, including PNGF, LCB1-PNGF as active editor, while empty vector and inactive mutant PNGF(D60N) as two negative controls. After 48 h of transfection, cells were incubated with 10 μM proteasome inhibitor MG132 (Salorbio, Beijing, China) for up to 12 h. Then cells were collected and lysed for western blotting. HEK293T-S1 stable cells were transiently transfected with indicated individual plasmid, such as PNGF, LCB1-PNGF, ScPNG1ΔH1, LCB1-ScPNG1ΔH1, as well as negative controls. After 48 h of transfection, cells were incubated with 10 μM proteasome inhibitor MG132 (Salorbio, Beijing, China) or 50 nM lysosome inhibitor NH_4Cl (Salorbio, Beijing, China) for up to 12 h. Then cells were collected and lysed for western blotting.

Flow Cytometry

HEK293T cells were transiently co-transfected with full-length wild-type spike-EGFP expressing plasmid and the editor plasmid PNGF or LCB1-PNGF, with an empty vector and an inactive mutant PNGF(D60N) as negative controls. After 48 h of transfection, cells were collected to detect the whole protein expression levels of spike by measuring EGFP mean fluorescence intensity using the flow cytometry instrument BD LSR Fortessa X-20 (BD Biosciences, California, USA). Cells expressing eGFP were gated, and the percentage depletion of GFP-positive cells was calculated relative to the control group. This experiment was performed in three biological replicates.

Cell–Cell Fusion Assay

Cell–cell fusion assays were performed following the protocol previously outlined [40], with some small modifications. In brief, HEK293T-S-WT stable cells were co-transfected with a plasmid encoding one of several spike deglycosylation editors and a pFR-Luc plasmid containing a synthetic promoter consisting of five tandem repeats of yeast GAL4 binding sites that regulate

Table 1. Key resources table

Reagent type (species) or resource	Designation	Source or reference	Identifiers	Additional information
Antibody	PD-L1/CD274 rabbit pAb	ABclonal (Hubei, China)	Cat#: A1645	WB (1:2000)
Antibody	PD-L1/CD274 rabbit mAb	ABclonal (Hubei, China)	Cat#: A19135	WB (1:2000)
Antibody	PD-1/CD279 rabbit pAb	ABclonal (Hubei, China)	Cat#: A11973	WB (1:2000)
Antibody	PD-1/CD279 rabbit pAb	ABclonal (Hubei, China)	Cat#: A5584	WB (1:2000)
Antibody	Influenza A H3N2 hemagglutinin/HA rabbit PAb	Sino Biological (Beijing, China)	Cat#: 11056-T62	WB (1:3000)
Antibody	Influenza A H3N2 hemagglutinin/HA mouse MAb	Sino Biological (Beijing, China)	Cat#: 11056-MM03	WB (1:2000)
Antibody	SARS-CoV-2 (2019-nCoV) spike RBD antibody, rabbit PAb	Sino Biological (Beijing, China)	Cat#: 40592-T62	WB (1:2000)
Antibody	SARS-CoV-2 (COVID-19) spike antibody, rabbit pAb	GeneTex (California, USA)	Cat#: GTX135356	WB (1:2000)
Antibody	Rabbit anti-p24 pAb	Sino Biological (Beijing, China)	Cat#: 11695-RP02	WB (1:2000)
Antibody	DDDDK-tag rabbit mAb	ABclonal (Hubei, China)	Cat#: AE092	WB (1:4000)
Antibody	Mouse anti DDDDK-tag mAb	ABclonal (Hubei, China)	Cat#: AE005	WB (1:4000)
Antibody	Vinculin rabbit mAb	ABclonal (Hubei, China)	Cat#: A23468	WB (1:4000)
Antibody	Rabbit anti HA-tag pAb	ABclonal (Hubei, China)	Cat#: AE036	WB (1:4000)
Antibody	HRP goat anti-rabbit IgG (H + L)	ABclonal (Hubei, China)	Cat#: AS014	WB (1:10000)
Antibody	HRP goat anti-mouse IgG (H + L)	ABclonal (Hubei, China)	Cat#: AS003	WB (1:10000)
Cell line (Homo Sapiens)	HEK293T	National Collection of Authenticated Cell Cultures (Shanghai, China)	Cat#: SCSP-502	
Cell line (Homo Sapiens)	HEK293T-hACE2	Sino Biological (Beijing, China)	Cat#: OEC001	
Cell line (Homo Sapiens)	Calu-3	iCell (Shanghai, China)	Cat#: iCell-h035	
Cell line (Homo Sapiens)	PC-9	National Collection of Authenticated Cell Cultures (Shanghai, China)	Cat#: SCSP-5085	

(*Continued on next page*)

Table 1. *Continued*

Reagent type (species) or resource	Designation	Source or reference	Identifiers	Additional information
Cell line (Homo Sapiens)	HEK293T-S-WT	This paper		
Cell line (Homo Sapiens)	HEK293T-S-Mutant	This paper		
Cell line (Homo Sapiens)	HEK293T-S-WT-EGFP	This paper		
Cell line (Homo Sapiens)	HEK293T-S1	This paper		
Recombinant DNA reagent	pcDNA3.1-PD-L1	GENEWIZ (Jiangsu, China)		Plasmid to express full length human PD-L1
Recombinant DNA reagent	pcDNA3.1-PD-1	GENEWIZ (Jiangsu, China)		Plasmid to express full length human PD-1
Recombinant DNA reagent	pcDNA3.1-H3N2-HA	GENEWIZ (Jiangsu, China)		Plasmid to express full length H3N2 hemagglutinin
Recombinant DNA reagent	pCDH-S-WT-EGFP	This paper	Derived from pcDNA3.1.2S [51]	Plasmid to express full length spike wild-type and EGFP
Recombinant DNA reagent	pCDH-S1-T2A-EGFP	This paper		Plasmid to generate HEK293T-spike S1 subunit cell line
Recombinant DNA reagent	pCDH-S-WT-T2A-EGFP	This paper		Plasmid to generate HEK293T-spike wild-type cell line
Recombinant DNA reagent	pCDH-S-Mutant-T2A-EGFP	This paper		Plasmid to generate HEK293T-spike mutant (^{682}'RRAR'^{685} mutated to 'GGSG' cell line
Recombinant DNA reagent	pcDNA3.1-S-WT-Δ19	This paper	[52]	Plasmid to express spike-Δ19 on viral coat
Recombinant DNA reagent	pLVX-IRES-ZsGreen1-Luc	HonorGene (Hunan, China)	Cat#: HG-VMH1035	
Recombinant DNA reagent	psPAX2	Addgene	Cat#: 12260	
Recombinant DNA reagent	VSV-G	Addgene	Cat#: 12259	
Recombinant DNA reagent	pFR-Luc	Hunan Fenghui Biotechnology (Hunan, China)	Cat#: QT019	
Recombinant DNA reagent	pBD–NF–κB	Hunan Fenghui Biotechnology (Hunan, China)	Cat#: QT016	

the expression of the luciferase gene. HEK293T-hACE2 stable cells were transfected with a pBD–NF–κB plasmid, which encodes a fusion protein containing the DNA binding domain of GAL4 and the transcription activation domain of NF-κB. After 40 h, an equivalent amount of different S-WT stable cells treated with various editors were detached using trypsin (0.25%) and plated on a 70% confluent monolayer of HEK293T-hACE2 stable cells at a 1:1 ratio. Following an incubation period of 16–

24 h, luciferase expression was activated when cell–cell fusion occurred between HEK293T-S-WT and HEK293T-hACE2 stable cells as the GAL4-NF-κB fusion protein bound to the GAL4 binding sites on the luciferase gene promoter. Each cell sample was lysed by adding 200 μL of firefly luciferase reporter gene assay cell lysis buffer (Beyotime, Shanghai, China) for 30 min, and the supernatants were obtained after centrifugation at 15,000 rpm for 5 min. Luciferase activity was then quantified using BrightLumi™ luciferase reporter gene assay kit (Beyotime, Shanghai, China) and measured with a BioTek Synergy Neo2 multimode microplate reader (BioTek Instruments, Inc., Vermont, USA). All experiments were performed in triplicate and repeated at least three times. To visualize the inhibition of deglycosylation-dependent protein editing on cell–cell fusion, HEK293T-S-WT-EGFP stable cells were transiently transfected with the pcDNA3.1-PNGF plasmid, the pcDNA3.1-LCB1-PNGF plasmid, as well as empty vector and inactive mutant PNGF(D60N) as negative controls. After 48 h of transfection, these pretreated HEK293T-S-WT-EGFP stable cells were detached using trypsin (0.25%) and plated on a 70%–80% confluent monolayer of HEK293T-hACE2 cells at a ratio of approximately 1:1. After 24 h of incubation, images of syncytia formation were captured using an OLYMPUS IX73 research inverted microscope with cellSens Entry software (Olympus Corporation, Tokyo, Japan).

Pseudovirus Production and Infection Assay

Pseudovirions were produced by co-transfection into HEK 293T cells with pLVX-IRES-ZsGreen1-Luc, psPAX2, and S-WT-Δ19, as well as either empty vector or LCB1-PNGF editor at a molar ratio of 1:1:2:1 by using polyetherimide (PEI). After 72 h of incubation, the supernatant media containing pseudovirions passed through a 0.45 μm filter and was centrifuged at 5000 rpm for 30 min at 4 °C to remove debris. The collected supernatants were concentrated with a universal virus concentration kit (Beyotime, Shanghai, China) and stored at −80 °C if necessary. The pseudoviral titers were determined using the Lentivirus Titer p24 ELISA Kit (Biodragon, Beijing, China) following the manufacturer's instructions. The concentration and deglycosylation state of viral spike glycoproteins were also verified by western blotting with anti-spike RBD pAb to detect equivalent amounts of the pseudovirions in each of the preparations with p24 as a loading control.

To measure the spike protein-mediated entry of pseudovirions, we utilized the commonly used HEK293T-hACE2, Calu-3, and PC-9 target cells. These cells were plated at approximately 25%–30% confluence in 96-well plates. The next day, the cells were exposed to 100 μL of 1:1 diluted pseudovirus. After 48 h of incubation, the cells were lysed using 100 μL of firefly luciferase reporter gene assay cell lysis buffer for 30 min. The resulting supernatant was obtained through centrifugation at 15,000 rpm for 5 min. Subsequently, 20 μL of each sample was combined with 100 μL of BrightLumi™ luciferase reaction reagent and incubated at RT for 5 min. The luciferase activity was quantified using a BioTek Synergy Neo2 multimode microplate reader.

Cell Viability Assay

HEK293T-S-WT stable cells were transiently transfected with the indicated plasmids. Following 48 h of transfection, the cells were gathered and quantified using the LUNAIITM automated cell counter. Subsequently, 40,000 cells from each sample were transferred into an opaque 96-well plate. Cell viability was assessed by adding 100 μL of CellTiter-Glo reagent (Promega, Wisconsin, USA) to each well and incubating it at RT for 10 min. The luminescence was then measured using a BioTek Synergy Neo2 multimode microplate reader.

Statistical Analysis

Statistical analysis (unpaired two-tailed Student's *t*-tests) was performed using GraphPad Prism 9 (GraphPad Software, Inc., La Jolla, USA). Data were derived from at least three independent biological replicate experiments and are presented as the mean ± standard deviation (SD); $^{*}P < 0.05$, $^{**}P < 0.01$, $^{***}P < 0.001$, and $^{****}P < 0.0001$.

ACKNOWLEDGMENTS

We thank Grammarly and ChatGPT for correcting grammar and improving readability in English writing. This work was supported by funding from the Key Project of the Ministry of Science and Technology of China (2018YFA0900500).

DECLARATION OF COMPETING INTERESTS

The authors declare that they have no known competing financial interests or personal relationships that could have appeared to influence the work reported in this paper.

ETHICS APPROVAL

Ethics approval is not required in this study.

AUTHOR CONTRIBUTIONS

Min Wu: writing – review & editing, writing – original draft, validation, investigation, formal analysis. **Guijie Bai:** writing – original draft, validation, investigation, formal analysis. **Ziyi Zhang:** writing – original draft, validation, investigation. **Haixia Xiao:** writing – review & editing, writing – original draft, resources. **Wenliang Sun:** supervision, resources, project administration. **Chaoguang Tian:** writing – review & editing, writing – original draft, supervision, project administration, funding acquisition, conceptualization.

DECLARATION OF GENERATIVE AI AND AI-ASSISTED TECHNOLOGIES IN THE WRITING PROCESS

During the preparation of this work, the authors only used ChatGPT-3.5 in order to improve readability and language. After using this tool, the authors reviewed and edited the content as needed and took full responsibility for the content of the publication.

SUPPLEMENTARY DATA

Supplementary data to this article can be found online at https://doi.org/10.1016/j.hlife.2024.07.003.

REFERENCES

[1] Anzalone AV, Koblan LW, Liu DR. Genome editing with CRISPR-Cas nucleases, base editors, transposases and prime editors. *Nat Biotechnol* 2020;38:824–44.
[2] Jinek M, Chylinski K, Fonfara I, Hauer M, Doudna JA, Charpentier E. A programmable dual-RNA-guided DNA endonuclease in adaptive bacterial immunity. *Science* 2012;337:816–21.

[3] Békés M, Langley DR, Crews CM. PROTAC targeted protein degraders: The past is prologue. *Nat Rev Drug Discov* 2022;21:181–200.
[4] Blum TR, Liu H, Packer MS, Xiong X, Lee PG, Zhang S, et al. Phage-assisted evolution of botulinum neurotoxin proteases with reprogrammed specificity. *Science* 2021;371:803–10.
[5] Ge Y, Ramirez DH, Yang B, D'Souza AK, Aonbangkhen C, Wong S, et al. Target protein deglycosylation in living cells by a nanobody-fused split O-GlcNAcase. *Nat Chem Biol* 2021;17:593–600.
[6] Pedram K, Shon DJ, Tender GS, Mantuano NR, Northey JJ, Metcalf KJ, et al. Design of a mucin-selective protease for targeted degradation of cancer-associated mucins. *Nat Biotechnol* 2024;42:597–607.
[7] Ruvkun G, Ji F, Sadreyev RI. Phylogenetic evidence for asparagine to aspartic acid protein editing of N-glycosylated SARS-CoV-2 viral proteins by NGLY1 deglycosylation/deamidation suggests an unusual vaccination strategy. bioRxiv (2021). 2021.09.11.459891.
[8] Lehrbach NJ, Breen PC, Ruvkun G. Protein sequence editing of SKN-1A/Nrf1 by peptide:N-glycanase controls proteasome gene expression. *Cell* 2019;177. 737-50.e15.
[9] Hirata T, Kizuka Y. N-Glycosylation. *Adv Exp Med Biol* 2021;1325:3–24.
[10] Esmail S, Manolson MF. Advances in understanding N-glycosylation structure, function, and regulation in health and disease. *Eur J Cell Biol* 2021;100:151186.
[11] Helenius A, Aebi M. Roles of N-linked glycans in the endoplasmic reticulum. *Annu Rev Biochem* 2004;73:1019–49.
[12] Sun L, Li CW, Chung EM, Yang R, Kim YS, Park AH, et al. Targeting glycosylated PD-1 Induces potent antitumor immunity. *Cancer Res* 2020;80:2298–310.
[13] Li CW, Lim SO, Xia W, Lee HH, Chan LC, Kuo CW, et al. Glycosylation and stabilization of programmed death ligand-1 suppresses T-cell activity. *Nat Commun* 2016;7:12632.
[14] Wang YN, Lee HH, Hsu JL, Yu D, Hung MC. The impact of PD-L1 N-linked glycosylation on cancer therapy and clinical diagnosis. *J Biomed Sci* 2020;27:77.
[15] Watanabe Y, Allen JD, Wrapp D, McLellan JS, Crispin M. Site-specific glycan analysis of the SARS-CoV-2 spike. *Science* 2020;369:330–3.
[16] Alymova IV, York IA, Air GM, Cipollo JF, Gulati S, Baranovich T, et al. Glycosylation changes in the globular head of H3N2 influenza hemagglutinin modulate receptor binding without affecting virus virulence. *Sci Rep* 2016;6:36216.
[17] Dugan AE, Peiffer AL, Kiessling LL. Advances in glycoscience to understand viral infection and colonization. *Nat Methods* 2022;19:384–7.
[18] Feng T, Zhang J, Chen Z, Pan W, Chen Z, Yan Y, et al. Glycosylation of viral proteins: implication in virus-host interaction and virulence. *Virulence* 2022;13:670–83.
[19] Vigerust DJ, Shepherd VL. Virus glycosylation: Role in virulence and immune interactions. *Trends Microbiol* 2007;15:211–8.
[20] Hoffmann D, Mereiter S, Jin Oh Y, Monteil V, Elder E, Zhu R, et al. Identification of lectin receptors for conserved SARS-CoV-2 glycosylation sites. *EMBO J* 2021;40:e108375.
[21] Huang HY, Liao HY, Chen X, Wang SW, Cheng CW, Shahed-Al-Mahmud M, et al. Vaccination with SARS-CoV-2 spike protein lacking glycan shields elicits enhanced protective responses in animal models. *Sci Transl Med* 2022;14:eabm0899.
[22] Yang Q, Kelkar A, Sriram A, Hombu R, Hughes TA, Neelamegham S. Role for N-glycans and calnexin-calreticulin chaperones in SARS-CoV-2 Spike maturation and viral infectivity. *Sci Adv* 2022;8:eabq8678.
[23] Huang HC, Lai YJ, Liao CC, Yang WF, Huang KB, Lee IJ, et al. Targeting conserved N-glycosylation blocks SARS-CoV-2 variant infection *in vitro*. *eBioMedicine* 2021;74:103712.
[24] Yang Q, Hughes TA, Kelkar A, Yu X, Cheng K, Park S, et al. Inhibition of SARS-CoV-2 viral entry upon blocking N- and O-glycan elaboration. *eLife* 2020;9:e61552.
[25] Casas-Sanchez A, Romero-Ramirez A, Hargreaves E, Ellis CC, Grajeda BI, Estevao IL, et al. Inhibition of protein N-glycosylation blocks SARS-CoV-2 infection. *mBio* 2021;13:e0371821.
[26] Suzuki T, Huang C, Fujihira H. The cytoplasmic peptide:N-glycanase (NGLY1) - structure, expression and cellular functions. *Gene* 2016;577:1–7.
[27] Sun G, Yu X, Bao C, Wang L, Li M, Gan J, et al. Identification and characterization of a novel prokaryotic peptide:N-glycosidase from *Elizabethkingia meningoseptica*. *J Biol Chem* 2015;290:7452–62.
[28] Joshi S, Katiyar S, Lennarz WJ. Misfolding of glycoproteins is a prerequisite for peptide:N-glycanase mediated deglycosylation. *FEBS Lett* 2005;579:823–6.
[29] Wang S, Xin F, Liu X, Wang Y, An Z, Qi Q, et al. N-terminal deletion of peptide:N-glycanase results in enhanced deglycosylation activity. *PLoS One* 2009;4:e8335.
[30] Wu Z, Cao Z, Yao H, Yan X, Xu W, Zhang M, et al. Coupled deglycosylation-ubiquitination cascade in regulating PD-1 degradation by MDM2. *Cell Rep* 2023;42:112693.
[31] Suzuki T. The cytoplasmic peptide:N-glycanase (Ngly1)-basic science encounters a human genetic disorder. *J Biochem* 2015;157:23–34.
[32] Park H, Suzuki T, Lennarz WJ. Identification of proteins that interact with mammalian peptide:N-glycanase and implicate this hydrolase in the proteasome-dependent pathway for protein degradation. *Proc Natl Acad Sci USA* 2001;98:11163–8.
[33] Bryan CM, Rocklin GJ, Bick MJ, Ford A, Majri-Morrison S, Kroll AV, et al. Computational design of a synthetic PD-1 agonist. *Proc Natl Acad Sci USA* 2021;118:e2102164118.
[34] Yin H, Zhou X, Huang YH, King GJ, Collins BM, Gao Y, et al. Rational design of potent peptide inhibitors of the PD-1:PD-L1 interaction for cancer immunotherapy. *J Am Chem Soc* 2021;143:18536–47.
[35] Chatterjee P, Ponnapati M, Kramme C, Plesa AM, Church GM, Jacobson JM. Targeted intracellular degradation of SARS-CoV-2 *via* computationally optimized peptide fusions. *Commun Biol* 2020;3:715.
[36] Cao L, Coventry B, Goreshnik I, Huang B, Sheffler W, Park JS, et al. Design of protein-binding proteins from the target structure alone. *Nature* 2022;605:551–60.
[37] Hirsch C, Blom D, Ploegh HL. A role for N-glycanase in the cytosolic turnover of glycoproteins. *EMBO J* 2003;22:1036–46.
[38] Cao L, Goreshnik I, Coventry B, Case JB, Miller L, Kozodoy L, et al. *De novo* design of picomolar SARS-CoV-2 miniprotein inhibitors. *Science* 2020;370:426–31.
[39] Huang J, Hou S, An J, Zhou C. In-depth characterization of protein N-glycosylation for a COVID-19 variant-design vaccine spike protein. *Anal Bioanal Chem* 2023;415:1455–64.
[40] Ou X, Zheng W, Shan Y, Mu Z, Dominguez SR, Holmes KV, et al. Identification of the fusion peptide-containing region in betacoronavirus spike glycoproteins. *J Virol* 2016;90:5586–600.
[41] Casalino L, Gaieb Z, Goldsmith JA, Hjorth CK, Dommer AC, Harbison AM, et al. Beyond shielding: the roles of glycans in the SARS-CoV-2 spike protein. *ACS Cent Sci* 2020;6:1722–34.
[42] Zheng L, Ma Y, Chen M, Wu G, Yan C, Zhang XE. SARS-CoV-2 spike protein receptor-binding domain N-glycans facilitate viral internalization in respiratory epithelial cells. *Biochem Biophys Res Commun* 2021;579:69–75.
[43] Harbison AM, Fogarty CA, Phung TK, Satheesan A, Schulz BL, Fadda E. Fine-tuning the spike: Role of the nature and topology of the glycan shield in the structure and dynamics of the SARS-CoV-2 S. *Chem Sci* 2022;13:386–95.
[44] Mori T, Jung J, Kobayashi C, Dokainish HM, Re S, Sugita Y. Elucidation of interactions regulating conformational stability and dynamics of SARS-CoV-2 S-protein. *Biophys J* 2021;120:1060–71.
[45] Sztain T, Ahn SH, Bogetti AT, Casalino L, Goldsmith JA, Seitz E, et al. A glycan gate controls opening of the SARS-CoV-2 spike protein. *Nat Chem* 2021;13:963–8.
[46] Zan F, Zhou Y, Chen T, Chen Y, Mu Z, Qian Z, et al. Stabilization of the metastable pre-fusion conformation of the SARS-CoV-2 spike glycoprotein through N-linked glycosylation of the S2 subunit. *Viruses* 2024;16:223.
[47] Tian W, Li D, Zhang N, Bai G, Yuan K, Xiao H, et al. O-glycosylation pattern of the SARS-CoV-2 spike protein reveals an "O-Follow-N" rule. *Cell Res* 2021;31:1123–5.
[48] Hu Z, Chen PH, Li W, Douglas T, Hines J, Liu Y, et al. Targeted dephosphorylation of tau by phosphorylation targeting chimeras (PhosTACs) as a therapeutic modality. *J Am Chem Soc* (2023). https://doi.org/10.1021/jacs.2c11706.
[49] Mei S, Ayala R, Ramarathinam SH, Illing PT, Faridi P, Song J, et al. Immunopeptidomic analysis reveals that deamidated HLA-bound peptides arise predominantly from deglycosylated precursors. *Mol Cell Proteomics* 2020;19:1236–47.
[50] Kuhn P, Guan C, Cui T, Tarentino AL, Plummer Jr TH, Van Roey P. Active site and oligosaccharide recognition residues of peptide-N4-(N-acetyl-beta-*D*-glucosaminyl)asparagine amidase F. *J Biol Chem* 1995;270:29493–7.
[51] Nie J, Li Q, Wu J, Zhao C, Hao H, Liu H, et al. Establishment and validation of a pseudovirus neutralization assay for SARS-CoV-2. *Emerg Microb Infect* 2020;9:680–6.
[52] Johnson MC, Lyddon TD, Suarez R, Salcedo B, LePique M, Graham M, et al. Optimized pseudotyping conditions for the SARS-COV-2 spike glycoprotein. *J Virol* 2020;94:e01062-20.